Determination of Temperatures within Acoustically Generated Bubbles in Aqueous Solutions at Different Ultrasound Frequencies

Envi Ciawi, James Rae, Muthupandian Ashokkumar, and Franz Grieser*

Particulate Fluids Processing Centre, School of Chemistry, University of Melbourne, Melbourne, Victoria 3010, Australia

Received: March 8, 2006; In Final Form: May 16, 2006

Mean acoustic bubble temperatures have been measured using a methyl radical recombination (MRR) method, at three ultrasound frequencies (20, 355, and 1056 kHz) in aqueous *tert*-butyl alcohol solutions (0−0.5 M). The method is based on yield measurements of some of the hydrocarbon products formed from the recombination of methyl radicals that are thermally generated within collapsing bubbles containing *tert*-butyl alcohol vapor. The mean bubble temperatures were found to decrease substantially with increasing *tert*-butyl alcohol concentration at 355 and 1056 kHz but only to a small extent at 20 kHz. Extrapolating the mean temperatures measured to zero concentration of *tert*-butyl alcohol, at a bulk solution temperature of 20 °C, gave the order 355 kHz (4300 ± 200 K) > 1056 kHz (3700 ± 200 K) > 20 kHz (3400 ± 200 K). It is also concluded that the temperature derived from the MRR method is a useful diagnostic parameter for sensing the thermal conditions within an active acoustic bubble. However, attention must be given to the fact that the temperature derived from the MRR method is not theoretically well defined.

Introduction

Sonochemistry is largely initiated by the violent collapse of microbubbles that are generated in a fluid exposed to high intensity ultrasound. Bubble collapse can occur so rapidly (less than a microsecond) that any gas and vapor trapped within the bubble is compressed, nearly adiabatically, to create a localized "hot spot" of several thousand degrees centigrade.[1] These temperatures are sufficiently high to generate radicals[2], excited-state species,[3−5] and in some instances meta-stable molecular ions,[6] within the bubble. All of these entities are capable of undergoing further reaction, such as with the various species within the bubble,[7] with solutes adsorbed at the bubble−solution interface,[7−9] and/or with solutes in bulk solution.[10,11]

There have been several methods reported to date for determining bubble temperatures in water[12−14] and in other fluids.[15,16] Recently, we applied[17] a relatively simple method for determining cavitation bubble temperatures in aqueous solutions, following a method originally introduced by Hart et al.[12] and then extended by Tauber et al.[8] The method is based on the competitive reaction pathways in the recombination of methyl radicals (MRR) as shown in Scheme 1.

The scheme shows that the recombination of methyl radicals can produce ethane and ethylene. Ethylene can be further thermally dehydrogenated to produce acetylene. Since acetylene is produced exclusively from ethylene, the ratio between the product yields of ethylene (plus acetylene) and ethane is equal to the ratio between the rate constants for the formation of ethylene and ethane, as shown in eq 1

$$[Y(C_2H_2 + C_2H_4)/Y(C_2H_6)] = k_{(C_2H_4)}/k_{(C_2H_6)} \qquad (1)$$

where Y equals the molar yield of each gas. As $k_{(C_2H_6)}$ is largely independent of temperature and $k_{(C_2H_4)}$ is sensitive to temperature,[12,18,19] a change in the ratio of the product yield reflects a change in the temperature at which the recombination reactions occur.

* Author to whom correspondence s hould be addressed. E-mail: franz@unimelb.edu.au.

SCHEME 1: Methyl Radical Recombination Reaction Pathways for the Formation of Acetylene, Ethylene, and Ethane

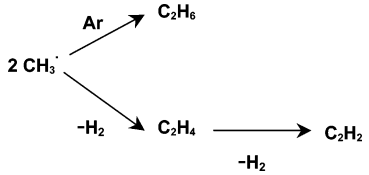

Tauber et al.[8] in their detailed study of the sonochemical decomposition of *tert*-butyl alcohol concluded from their extensive product analysis results that the main decomposition pathway for the alcohol was through thermolysis, yielding methyl radicals via the reaction

$$(CH_3)_3COH \rightarrow 3CH_3 + CO + H \qquad (2)$$

In the present study we have made use of *tert*-butyl alcohol as a methyl radical source and the MRR method to examine the temperatures realized within cavitation bubbles generated at different ultrasound frequencies and at different bulk solution temperatures. We have also examined the effects of sonication time and the solution concentration of *tert*-butyl alcohol on the temperatures determined by the MRR method.

Experimental Details

Samples were prepared with solute concentrations of between 0 and 500 mM. All solutions were prepared using Milli-Q (Millipore) water. Solutions were prepared to a total volume of 10 mL and placed in 15 mL vials fitted with septa. Prior to sonication samples were purged with argon by bubbling the gas through for a period of 5 min. For 355 and 1056 kHz experiments a laboratory sonicator (ELAC model USW 51-052) was used. The sonicator was filled with 200 mL of Milli-Q (Millipore) water and cooled during sonication by running water through an external reservoir at an approximate rate of 3−4 dm^3/min. Sample vials were placed in duplicate into the water-

10.1021/jp061441t CCC: $33.50
Published on Web 06/17/2006

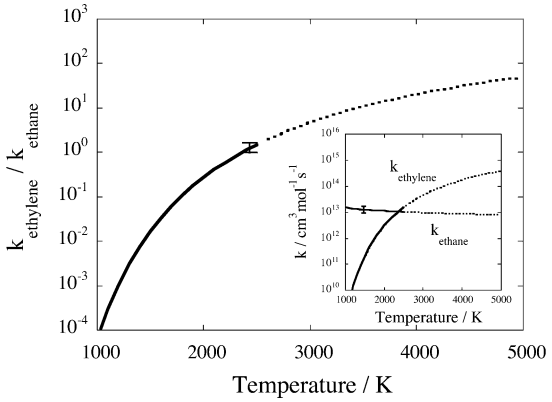

Figure 1. Ratio of rate constants, $k_{(C_2H_4)}/k_{(C_2H_6)}$ (equal to the ratio of the hydrocarbon gas product yields as defined in the text) as a function of temperature. Inset: Temperature dependence of the rate constants, $k_{(C_2H_4)} = 1.0 \times 10^{16} \exp(-134\ \text{kJ}/RT)$ and $k_{(C_2H_6)} = 2.4 \times 10^{14}\ T^{-0.4}$. The dashed portions of the curves in the figure indicate the regions of extrapolation of the functions defining the rate constants.[18,19]

filled sonication cell. They were positioned vertically through holes in a fitted lid and held in place with rubber O-rings. A power setting of 50 W was used; this corresponded to an actual power delivery of 28 W determined by calorimetry measurements on 200 mL of Milli-Q water in the sonication cell. Unless otherwise specified, 355 kHz samples were sonicated for 15 min, 1056 kHz samples for 30 min.

For 20 kHz samples a laboratory cup−horn sonicator (Branson Ultrasonics 20 kHz transducer) was used. Samples were prepared as above and sonicated individually at a similar power (power setting = 120 W; calorimetric power = 28 W) to that used for the other frequencies for 60 min.

The yields of methane, ethane, ethylene, and acetylene were determined by gas chromatography. A gas chromatograph (Shimadzu GC-17A) with a flame ionization detector and a methyl silicone gum column (J&W Scientific) was used. Two 100 μL aliquots were taken from the headspace of each sample and analyzed. Product yields were then averaged over the injections and corrected for solubility of the gases in solution. Calibration curves were constructed for each gas by injecting known amounts into the column. Through the use of these calibration curves product yields were determined by converting the peak areas into gas concentrations. (Note that the reason for using the different sonication times for the three frequencies was to make sure that the level of products formed was sufficient to minimize measuring errors.)

Bubble temperatures were calculated from the following ratio

$$r = [Y(C_2H_2) + Y(C_2H_4)]/Y(C_2H_6) \qquad (3)$$

where Y is the corrected yield of each gas.[17] The corresponding temperatures were obtained from Figure 1. It should be noted that the rate constants used in the calculations have only been experimentally determined for the temperature ranges indicated (bold lines) in the figure. However, considering the monotonic quality of the functions the extrapolations are not likely to be greatly in error. The error bar shown in the figure is taken from an estimate of the reliability of the determined rate constants, and this is based on a critical evaluation of the literature on the reaction examined.[18,19]

Results

Examples of the yields of the main hydrocarbon products produced from the sonication of *tert*-butyl alcohol solutions at 20, 355, and 1056 kHz are given in Figure 2. The data were collected at approximately the same power levels delivered into the solutions surrounding the sealed reaction vials containing the various, argon-saturated, *tert*-butyl alcohol solutions.

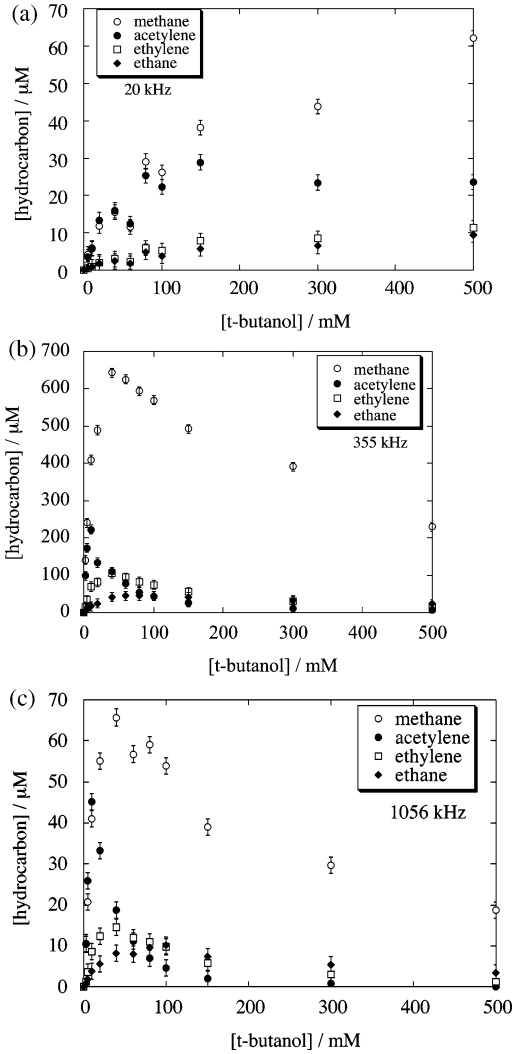

Figure 2. Methane, ethane, ethylene, and acetylene yields produced from the sonication of argon-saturated of *tert*-butyl alcohol solutions at (a) 20 kHz for 60 min, (b) 355 kHz for 15 min, and (c) 1056 kHz for 30 min and at a bulk solution temperature of 20 °C.

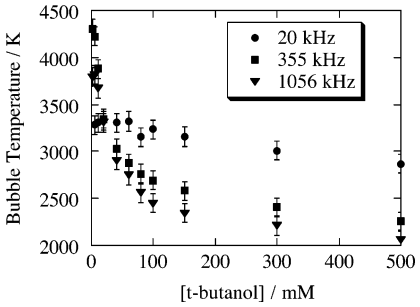

Figure 3. Bubble temperatures in aqueous *tert*-butyl alcohol solutions determined using the data from Figure 2 and the calibration curve presented in Figure 1.

On the basis of the equations given in the Experimental Section and the calculations presented in Figure 1, the data from Figure 2 were converted to temperatures, and these results are given in Figure 3. Similar experiments as those carried out to obtain Figure 2 were also conducted at a solution temperature of 40 °C, and the subsequently determined temperatures are shown in Figure 4.

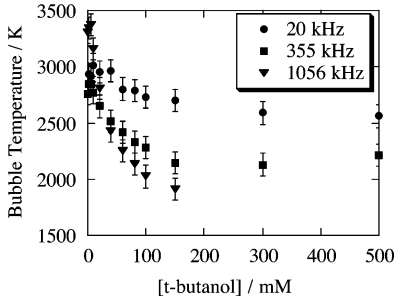

Figure 4. Bubble temperatures in argon-saturated aqueous *tert*-butyl alcohol solutions determined at a bulk solution temperature of 40 °C at (a) 20 kHz for 60 min, (b) 355 kHz for 15 min, and (c) 1056 kHz for 30 min.

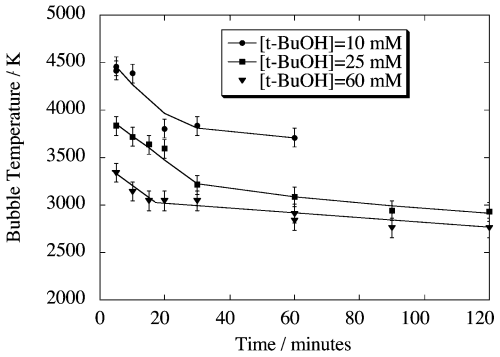

Figure 5. Bubble temperatures in argon-saturated aqueous *tert*-butyl alcohol solutions determined at three different *tert*-butyl alcohol concentrations, as a function of sonication time at an ultrasound frequency of 355 kHz and a bulk solution temperature of 20 °C.

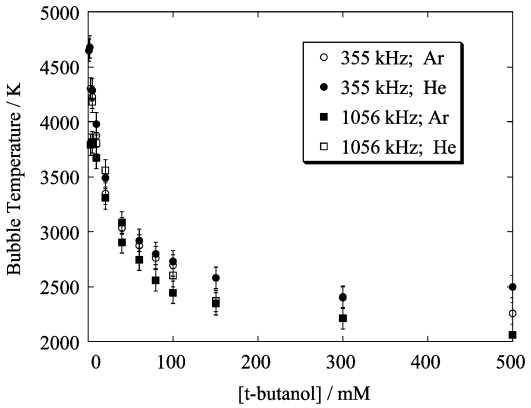

Figure 6. Comparison of bubble temperatures from the sonication of argon- and helium-saturated *tert*-butyl alcohol solutions at 355 and 1056 kHz at a bulk solution temperature of 20 °C.

In another series of experiments the acoustic bubble temperatures were determined for different lengths of sonication time at different concentrations of *tert*-butyl alcohol, and the results are shown in Figure 5.

Finally, the effect of using helium as the saturating gas was compared with the argon systems, and these results are shown in Figure 6.

Discussion

The MRR method involves a number of assumptions, and these have been discussed at some length by Hart et al.[12] and by Tauber et al.[8] The four most significant assumptions are:

(i) It must be accepted that the rate constants for ethane and ethylene production, as depicted by Scheme 1, are valid for the conditions experienced during bubble collapse.

(ii) The methyl radical is the dominant intermediate species through which ethane and ethylene are produced.

(iii) Acetylene is predominantly produced through the thermal dehydrogenation of ethylene.

(iv) No significant side reactions involving the products take place, or if side reactions are significant, then ethane, ethylene, or acetylene are not disproportionately depleted or created.

As indicated in our previous study[17] on bubble temperature determinations by the MRR method, it is difficult to directly verify the above assumptions. However, it was noted that the temperatures determined by the MRR method, under the conditions used, were comparable to the values determined by other, quite different methods.[13,14] This outcome would suggest that the assumptions are valid. Furthermore, from the results of our previous study[17] it could be inferred that assumptions i−iv are valid for the MRR method, in that it was found that almost the same cavitation bubble temperatures were determined regardless of the primary source of the methyl radials. This would not be expected to be the case if side reactions interfered with the primary reaction pathways of the methyl radical, as given by Scheme 1. This was also noted by Tauber et al.[8]

Another point that needs to be addressed, before the results are discussed, is the issue of what actually is the temperature being measured. It is theoretically understood[1,20,21] that the temperature within the bubble will be constantly changing as the radius of the bubble decreases during the bubble collapse. It is useful to identify three distinct volume regions within the core of a bubble in discussing the bubble temperature: (1) the bubble−solution interfacial region, where it can be expected that the temperatures are much cooler than further into the bubble core;[20] (2) the region away from the interface and extending toward the center of the collapsing bubble, where the temperature is likely to be uniform as suggested by the theoretical work of Storey and Szeri[21] and higher than that at the edge of the bubble solution interface; (3) the very core of the bubble, where conditions may yield temperatures sufficiently high to produce a plasma, and probably the region where broad wavelength sonoluminescence arises.[22]

As already stated above, not only will there be a regional difference in temperature within the collapsing bubble but also a temporal one as the radius of the bubble diminishes. It is not until the temperatures are sufficiently high, such that methyl radicals are produced, that a "chemical" temperature, with respect to the MRR method, can be accessed. If temperatures are reached that decompose the methyl radical, then the MRR method will of course not reveal these conditions. Strictly therefore, the MRR method reports on the temperature in all regions within the bubble and during the time that methyl radicals are produced and remain thermally stable.

It is instructive to explore this temporal domain further. Giri and Arakeri[23] reported the duration of the light emitted from electronically excited sodium atoms (Na*), from argon-saturated aqueous NaCl solutions, to be about 100 ns. This time, as they pointed out, far exceeds the emission lifetime of Na*, and therefore it can be taken that the emission time reflects the period in which thermal processes are taking place to chemically generate excited sodium atoms. This time is relatively long, and the temperature profile within a single bubble would range widely between the beginning and the end of this 100 ns interval. If it is assumed that a similar time period exists for the formation and reaction of the methyl radical, then the temperature accessed by the MRR method would then be a mean temperature characterizing the thermal conditions experienced by the chemical reactions in the bubble over a relatively long period of time during bubble collapse.

It can also be argued that the temperature obtained by the MRR method would be biased to the higher temperatures of the collapse period. There are two main reasons this would be the case. First, the reaction rate constant for ethylene formation increases with increasing temperature. Therefore, for any given concentration of methyl radicals more ethylene would be produced in a given time period at the higher temperatures than at the lower temperatures. On product analysis this rate constant effect would favor a higher temperature determination. Second, during the time interval where the higher temperatures are reached within the bubble the concentration of methyl radicals would be higher than that at lower temperatures. This would occur not only because relatively more methyl radicals would be produced thermally at the higher temperatures but also because they would be produced in a smaller volume. The consequence of this is that the integrated product yields would again reflect the relatively higher yields produced at the higher temperatures.

The above discussion sets the scene for examining the temperature trends revealed in the data presented in the results section. It can be seen in Figure 2 that the yield profiles of the hydrocarbon (HC) gases produced at 355 and 1056 kHz, as a function of *tert*-butyl alcohol, are quite similar but vary significantly from the 20 kHz results. The reason for this will be addressed below. For the two higher frequencies, it can also be noted that at very low concentrations of *tert*-butyl alcohol the yields of HC increase almost linearly with increasing concentration of *tert*-butyl alcohol. At *tert*-butyl alcohol concentrations of around 40 mM all the HC gases have passed through a maximum yield and then decline in yield at higher *tert*-butyl alcohol levels. These observations may be interpreted in several ways, and therefore it is prudent to leave further discussion until after the data of Figure 3 are considered.

The temperature calculations show that for sonication at both 355 and 1056 kHz there is a drop of over 2000 K in the mean bubble temperature in the range of *tert*-butyl alcohol concentrations studied, whereas for 20 kHz the temperature drop is only slight, on the order of a few hundred Kelvin. These observations help in qualitatively interpreting the results of Figure 2. As the *tert*-butyl alcohol concentration increases more alcohol will evaporate into the bubble, as has been discussed previously,[17] thereby increasing the heat capacity of the core as well as providing an increase in the number of molecules that can be thermally decomposed (endothermic processes). The two competing processes, one producing more methyl radicals than the other, as a consequence of the decreasing mean core temperature, reducing the number of methyl radicals, can account for the product maxima in Figures 2b and 2c.

The difference in the extent of the reduction in temperature at higher *tert*-butyl alcohol concentrations between the 20 kHz system and the other two higher frequencies requires an additional condition to exist. We have concluded from several studies on sonoluminescence quenching by alcohols over a range of frequencies that under the conditions used in this study, at 20 kHz the active cavitation bubbles (i.e., those bubbles that produce sonoluminescence) undergo only a few oscillations, whereas at the higher frequencies the active bubbles are likely to oscillate several thousand times.[24−26] This means that at the higher frequencies there is a buildup of alcohol and gaseous HC products within an active bubble core, all of which go toward lowering the mean bubble temperature. In contrast, at 20 kHz because of the fewer oscillations that an active bubble experiences this cannot occur, and hence the mean core temperature is hardly affected by the alcohol content of the system.

On the basis of the model above, it follows that by extrapolating the bubble temperatures of Figure 3 to zero *tert*-butyl alcohol concentration an estimate of the mean bubble temperature when only argon and water vapor would be present in the bubble core can be made. Interestingly, the extrapolated temperatures are dependent on the sonication frequency. Perhaps surprisingly the extrapolated temperature for the 20 kHz system of 3400 K is significantly lower than that at the higher frequency. It would at first be expected that because the resonance radius, and also the maximum radius of expansion, of a 20 kHz bubble is considerably larger than that for the higher frequencies the collapse would generate a higher core temperature, not a lower one as measured. However, there are likely to be other factors that come into play that will determine the mean bubble temperature. For example, it needs to be remembered that at 20 kHz the time taken for the bubble to grow to its maximum size is considerably longer (15−50 times longer) than at the higher frequencies. During this expansion time water vapor will be continuously drawn into the bubble. As a consequence of this there will be more material inside the bubble that can take up the mechanical energy of the collapse and thereby moderate the temperature generated.

The results of Figure 4 support the interpretations discussed above. The extrapolated mean bubble temperatures at all frequencies are lower at a bulk water temperature of 40 °C compared with the values at 20 °C. As the water vapor pressure at 40 °C is almost 3 times that at 20 °C it can be expected that higher levels of water vapor within the bubble at the higher temperature would reduce the core temperature of the bubble. That the effect is not more pronounced, considering the large difference in the vapor pressures at the two bulk temperatures (6.7 kPa cf. 2.7 kPa), possibly reflects the nonequilibrium conditions that exist during bubble expansion and collapse.

The results of Figures 5 and 6 lend strong support to the idea that it is HC product buildup, within the higher-frequency active bubbles, that is responsible for the lowering of the mean core temperature of the bubbles at increasing alcohol levels. The data presented in Figure 5 reveal the significant observation that the shorter the sonication time the higher the temperature measured at any given alcohol level. This can only be the case if the products themselves contribute to the lowering of the bubble temperature. Any possible contribution to the effect being due to the inert gas in the system is ruled out by the near identical results of the argon and helium system comparisons at 355 and 1056 kHz shown in Figure 6.

One further point to comment on in Figure 5 is the leveling off of the determined temperature at longer sonication times. This suggests that some balance or steady-state-like condition is reached between HC being produced and incorporated within the bubble and HC being removed from the bubble. The adsorption of alcohol at the bubble−solution interface, the evaporation of the alcohol into the bubble during the expansion phase of the bubble oscillations, as well as the expulsion of alcohol and HC products into bulk solution during the compression phases will all be involved in achieving the steady-state condition. The extent of these mass transport processes will in turn depend on the number of oscillations an active bubble undergoes as well as the volume changes it experiences during its lifetime.

In summary it can be said that the MRR method provides a diagnostic mean bubble temperature that reflects the temperature

conditions at which sonochemical reactions occur within a bubble core. The temperature measured by the method does not report a maximum nor a minimum bubble temperature but rather an ill-defined mean temperature that remains to be theoretically identified. The results also indicate that the mean core temperature is dependent on the ultrasound frequency being applied to the solution. The mean temperature within a bubble in argon-saturated water, found by extrapolating the temperature results at a bulk solution temperature of 20 °C to zero *tert*-butyl alcohol concentrations, at the different ultrasound frequencies examined, follows the order 355 kHz (4300 ± 200 K) > 1056 kHz (3700 ± 200 K) > 20 kHz (3400 ± 200 K). It now remains to develop a theoretical understanding of these results.

Acknowledgment. Support from the Australian Research Council, the Particulate Fluids Processing Centre, and The University of Melbourne is gratefully acknowledged. E.C. also acknowledges a Melbourne University Postgraduate Research Scholarship.

References and Notes

(1) (a) Leighton, T. G. *The Acoustic Bubble*; Academic Press: London, 1994. (b) *Sonochemistry and Sonoluminescence*; Crum, L. A., Mason, T. J., Reisse, J. L., Suslick, K. S., Eds.; NATO ASI Series, Series C, Mathematical and Physical Sciences 524; Kluwer Academic Publications: Dordrecht, The Netherlands, 1999.

(2) Riesz, P.; Kondo, T. *Free Radical Biol. Med.* **1992**, *13*, 247.

(3) Flint, E. B.; Suslick, K. S. *J. Am. Chem. Soc.* **1989**, *111*, 6987.

(4) Lepoint-Mulie, F.; Voglet, N.; Lepoint, T.; Avni, R. *Ultrason. Sonochem.* **2001**, *8*, 151.

(5) Sehgal, C.; Sutherland, R. G.; Verrall, R. E. *J. Phys. Chem.* **1980**, *84*, 388.

(6) Flannigan, D. J.; Suslick, K. S. *Nature* **2005**, *434*, 52.

(7) Henglein, A. *Adv. Sonochem.* **1993**, *3*, 17.

(8) Tauber, A.; Mark, G.; Schuchmann, H.-P.; von Sonntag, C. *J. Chem. Soc., Perkin Trans. 2* **1999**, *2*, 1129.

(9) Sostaric, J. Z.; Mulvaney, P.; Grieser, F. *J. Chem. Soc., Faraday Trans.* **1998**, *91*, 2843.

(10) Caruso, R. A.; Ashokkumar, M.; Grieser, F. *Langmuir* **2002**, *18*, 7831.

(11) Bradley, M.; Grieser, F. *J. Colloid Interface Sci.* **2002**, *251*, 78.

(12) Hart, E. J.; Fischer, C.-H.; Henglein, A. *Radiat. Phys. Chem.* **1990**, *36*, 511.

(13) Misik, V.; Miyoshi, N.; Riesz, P. *J. Phys. Chem.* **1995**, *99*, 3605.

(14) Didenko, Y. T.; McNamara, W. B., III.; Suslick, K. S. *J. Am. Chem. Soc.* **1999**, *121*, 5817.

(15) Suslick, K. S.; Hammerton, D. A.; Cline, R. E., Jr. *J. Am. Chem. Soc.* **1986**, *108*, 5641.

(16) Didenko, Y. T.; McNamara, W. B., III.; Suslick, K. S. *Phys. Rev. Lett.* **2000**, *84*, 777.

(17) Rae, J.; Ashokkumar, M.; Eulaerts, O.; von Sonntag, C.; Reisse, J.; Grieser, F. *Ultrason. Sonochem.* **2005**, *12*, 325.

(18) Tsang, W.; Hampson, R. F. *J. Phys. Chem. Ref. Data* **1986**, *15*, 1087.

(19) Warnatz, J. *Combustion Chemistry*; Springer: Berlin, 1984.

(20) Yasui, K. *J. Chem. Phys.* **2002**, *116*, 2945.

(21) Storey, B. D.; Szeri, A. J. *J. Fluid Mech.* **1999**, *396*, 203.

(22) Ashokkumar, M.; Grieser, F. *J. Am. Chem. Soc.* **2005**, *127*, 5326.

(23) Giri, A.; Arakeri, V. H. *Phys. Rev. E.* **1998**, *58*, 2713.

(24) Ashokkumar, M.; Mulvaney; P.; Grieser, F. *J. Am. Chem. Soc.* **1999**, *121*, 7355

(25) Tronson, R.; Ashokkumar, M.; Grieser, F. *J. Phys. Chem. B* **2003**, *107*, 7307.

(26) Price, G. J.; Ashokkumar, M.; Hodnett, M.; Zequiri, B.; Grieser, F. *J. Phys. Chem. B* **2005**, *109*, 17799.